Temperature-dependent electron and hole transport in disordered semiconducting polymers: Analysis of energetic disorder

J. C. Blakesley,* H. S. Clubb, and N. C. Greenham
Cavendish Laboratory, J. J. Thomson Avenue, Cambridge CB3 0HE, United Kingdom
(Received 21 October 2009; revised manuscript received 9 December 2009; published 29 January 2010)

We have used space-charge limited current measurements to study the mobility of holes and electrons in two fluorene-based copolymers for temperatures from 100 to 300 K. Interpreting the results using the standard analytical model produced an Arrhenius-type temperature dependence for a limited temperature range only and mobility was found to be apparently dependent on the thickness of the polymer film. To improve on this, we have interpreted our data using a numerical model that takes into account the effects of the carrier concentration and energetic disorder on transport. This accounted for the thickness dependence and gave a more consistent temperature dependence across the full range of temperatures, giving support to the extended Gaussian disorder model for transport in disordered polymers. Furthermore, we find that the same model adequately describes both electron and hole transport without the need to explicitly include a distribution of electron traps. Room-temperature mobilities were found to be in the region of 4×10^{-8} and 2×10^{-8} $cm^2\,V^{-1}\,s^{-1}$ in the limit of zero field and zero carrier density with disorders of 110 ± 10 and 100 ± 10 meV for polymers poly{9,9-dioctylfluorene-co-bis[*N*,*N*′-(4-butylphenyl)]bis(*N*,*N*′-phenyl-1,4-phenylene)diamine} and poly(9,9-dioctylfluorene-co-benzothiadiazole), respectively.

DOI: 10.1103/PhysRevB.81.045210 PACS number(s): 72.80.Le, 73.61.Ph, 73.40.Sx, 85.30.De

I. INTRODUCTION

Charge-carrier transport in many disordered organic semiconductors and, in particular, conjugated polymers occurs by thermally assisted tunneling via highly localized states and is consequently strongly temperature dependent. In contrast to the bandlike transport seen in many inorganic crystals, this leads to room-temperature mobilities that are small enough to be a limiting factor in the performance of devices such as organic light-emitting diodes (OLEDs) and organic photovoltaics (OPVs). In the case of OLEDs, much theoretical work has been carried out to model charge transport and its effect on efficiency.[1] Generally, larger luminances can be achieved when electron and hole mobilities are large and well balanced. It has also been shown that the efficiency of OPVs may be limited by the rate at which photogenerated carriers can be extracted from organic layers.[2] Therefore, a proper description of charge transport in organic semiconductors is necessary for understanding device performance. Despite this, there is still no consensus on the most appropriate way to do this. In particular, it is not clear whether charge transport is limited by trapping, energetic disorder, or polaronic effects. Variations in electron transport between different conjugated copolymers have been attributed to the trapping effects of impurities introduced during synthesis.[3] Previous studies of electron currents in conjugated polymers have included specific modeling of shallow traps[4] or traps combined with energetic disorder[5] in order to account for apparent temperature and thickness dependence of mobility, with such models giving good agreement with experimental measurements. The latter of these studies reconciles the difference in electron and hole mobilities in a derivative of poly(phenylene vinylene) by assuming that electron transport is limited by charge trapping. However, models based solely on energetic disorder can also account for such effects as they implicitly include a number of low-energy states that effectively act as trapping centers.

In this paper, we focus on using energetic disorder as a method for modeling charge transport, showing that materials can be described simply by a single value of energetic disorder, without needing to refer to an explicit distribution of trap states. Furthermore we show that the same model can be used for both positive and negative charge carriers in conjugated polymers, leading to simplified modeling of bipolar devices.

II. THEORY OF SPACE-CHARGE LIMITED CURRENTS

The polymers used is this work, poly{9,9-dioctylfluorene-co-bis[*N*,*N*′-(4-butylphenyl)]bis(*N*,*N*′-phenyl-1,4-phenylene)diamine} (PFB) and poly(9,9-dioctylfluorene-co-benzothiadiazole) (F8BT) (see Fig. 1 for chemical structure) are air-stable polymers based on polyfluorene. The fluorene units are copolymerized with hole- or electron-transporting units, respectively. These polymers have been widely investigated for their use in both OLEDs (Ref. 6) and all-polymer OPVs,[7] and are a useful materials system for studying the physics of polymer devices.

Since most OLED and OPV devices consist of one or more thin (on the order of 100 nm) layers of active material

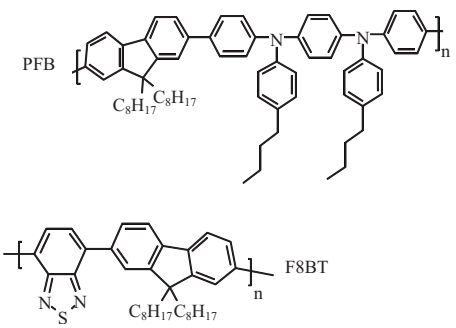

FIG. 1. Chemical structure of PFB and F8BT.

sandwiched between metal contacts, it is appropriate to measure the mobility in devices with a similar configuration. Therefore charge transport is investigated using steady-state current-voltage (*J-V*) measurements. This is achieved by selecting metal contacts such that only holes (electrons) are injected into the active layer. A build up of positive (negative) charge in the active layer then limits the total current density. Such a device is called space-charge limited (SCL). At the simplest level, *J-V* curves in single-carrier SCL devices can be interpreted by assuming a constant mobility and fitting[8] with the Mott-Gurney relation[9]

$$J = \frac{9}{8}\mu\varepsilon\frac{V^2}{d^3}, \tag{1}$$

where J is the current density, V is the applied voltage (taking account of any built-in voltage), μ is the mobility, ε is the permittivity of the material, and d is the film thickness. It has been shown that this is an oversimplification as studies using time-of-flight,[10–12] SCL current,[13] dark injection, and admittance spectroscopy[14] have all shown that mobility tends to change with the application of an electric field in organic semiconductors. The field dependence of mobility has often been described by a Poole-Frenkel-type enhancement factor,

$$g_1(E,T) = \exp[\gamma(T)\sqrt{E}], \tag{2}$$

where E is the electric field and $\gamma(T)$ is a materials parameter reflecting the strength of the electric field dependence. This parameter is generally found to decrease with increasing temperature, T. A modified version of the Mott-Gurney equation by Murgatroyd[15] is used to describe the *J-V* characteristics of SCL devices with Poole-Frenkel-type mobility enhancement,[7,16]

$$J = \frac{9}{8}\mu_0\varepsilon\,\exp(0.89\gamma\sqrt{V/d})\frac{V^2}{d^3}. \tag{3}$$

More recently, Tanase *et al.*[17] considered the effect of carrier concentration on mobility. Devices with large carrier concentrations, such as field-effect transistors, were found to have much higher mobility than those with low carrier concentrations. They demonstrated that the effect of carrier concentration can be understood by including a second mobility enhancement factor. Thus, rather than describing transport by a constant mobility, it is more appropriate to consider mobility as a function of a number of parameters,

$$\mu(T,E,n) = \mu_0(T)g_1(E,T)g_2(n,T), \tag{4}$$

where g_1 and g_2 are the dimensionless mobility enhancement factors for electric field, E, and carrier density n, respectively. μ_0 is the mobility as a function of temperature, T, in the low-field, low-carrier-density limit.

Modeling studies of charge transport have been carried out in the framework of the Gaussian disorder model (GDM) pioneered by Bässler.[18] A fundamental assumption of this model is that carriers are highly localized to specific fixed sites within a medium. Carriers hop between these sites, which each have a random energy offset taken from a Gaussian distribution. The width (standard deviation) of the Gaussian, σ, quantifies the amount of energetic disorder in the material. Bässler's Monte Carlo simulations of transport have successfully described the field-dependent mobility enhancement observed in experiments. However, Monte Carlo simulations become more computationally intensive as the carrier density is increased, so they are generally carried out in the limit of low carrier densities, which gives no information on the second mobility enhancement factor. Instead, numerical[19] and analytical[20] models have been used to make predictions about the carrier-density dependence of mobility.

Of these two models, the Pasveer model,[19] which is referred to as the extended Gaussian disorder model (EGDM), obtains mobility functions by solving carrier transport in a three-dimensional medium with Gaussian disorder using a master-equation approach. This approach allows the simulation of large carrier densities without the computational overheads experienced with Monte Carlo simulations. The mobility is then parameterized using a simple equation that allows a rapid approximation of the mobility enhancement factors, g_1 and g_2 without the need for detailed modeling. The Fishchuk model[20] instead uses an analytical model to derive the mobility as a function of carrier density. This model involves integrating a hopping rate over the density of occupied and unoccupied states. Unlike the Pasveer model, the Fishchuk model does not derive mobility as a function of electric field.

Both of these models give similar results, predicting a constant mobility at low carrier concentrations with a strong enhancement when the carrier concentration exceeds a certain level. This critical concentration corresponds to the density at which carriers essentially cease to behave independently of one another. The mobility enhancement is dependent on the ratio σ/k_BT (referred to as $\hat{\sigma}$), with stronger enhancement occurring as disorder is increased or temperature is reduced. The reason for the mobility enhancement with carrier concentration is easy to understand. The Gaussian density of states includes a low-energy tail of states extending well below the mean site energy. Carriers in these low-energy sites are effectively trapped since the surrounding sites are likely to have higher energies and hence the carriers require significant thermal activation to hop to a neighboring site. At low carrier concentrations, carriers predominantly occupy the low-energy sites and thus the mobility is low. When the carrier concentration exceeds a critical value, the tail of the density of states is effectively filled and any new carriers added to the system must occupy higher-energy states from which hopping is easier, leading to an increased mobility.

The temperature dependence of mobility is a critical factor in understanding the physics underlying charge transport. All three models mentioned above (Bässler, Pasveer, and Fishchuk) based on the GDM predict the logarithm of mobility will vary as $\hat{\sigma}^2$ in the low-carrier-density limit. Contradictorily, many studies of mobility in SCL devices[21] show an apparent temperature dependence closer to $1/T$. Rather than contradicting the GDM, this temperature dependence has been attributed to the effects of carrier density,[22] which can typically be on the order of 10^{16}–10^{18} cm^{-3} in SCL devices. Indeed, Fishchuk[20] has shown that the effective mobility is expected to follow this behavior at high carrier densities.

Therefore, to completely understand experimental data, it is necessary that the next generation of device simulations

include both field and concentration contributions to mobility. van Mensfoort and Coehoorn[22] have recently included these effects (using the Pasveer[19] model) within a one-dimensional continuum device model. The model has been used to fit *J-V* curves of hole transport in a conjugated polymer[23] and successfully described the temperature and film thickness dependence. By the inclusion of the concentration effects, the predicted $\hat{\sigma}$ dependence was reproduced. In this paper, we use a similar device simulation to investigate charge transport in films of PFB and F8BT. We also compare the effects of interchanging the Fishchuk model and Pasveer model for carrier-density dependence and of using a Poole-Frenkel field dependence. Although detailed simulations have shown that transport in disordered materials occurs through a three-dimensional network of microscopic filaments, a recent study has shown that the use of such one-dimensional continuum models is justified as long as the material thickness is greater than the typical filament size.[24] In practice, all SCL devices are likely to fall into this category.

III. EXPERIMENTAL METHOD

Single-carrier devices were fabricated by spin-coating PFB and F8BT from solution in *p*-xylene. Indium-tin oxide (ITO) coated glass was used for substrates. Substrates were cleaned ultrasonically in acetone then propan-2-ol, then treated with an oxygen plasma. For PFB, hole-only devices were fabricated by spin-coating poly(3,4-ethylene dioxythiophene) doped with poly(styrene sulfonate) as the bottom, hole-injecting electrode. PFB was spin coated in ambient conditions, then gold was evaporated to form the top electrode. For F8BT devices, the ITO coating was first removed from the substrate by etching in HCl prior to cleaning. Aluminum was evaporated onto the glass to create a bottom contact. The aluminum-coated substrates remained in a protective nitrogen environment while F8BT was spin coated. Finally, calcium capped with aluminum was evaporated as an electron-injecting top electrode. For each polymer, devices of three different thicknesses ranging from 50 to 350 nm were fabricated by varying the concentration of the polymer solutions. Film thicknesses were measured using a Dektak surface profiler. Devices were mounted in a liquid-helium cryostat and steady-state current-voltage characterization was carried out using a Keithley 6487 electrometer at temperatures ranging from 100 to 295 K. Care was taken to ensure that steady-state current measurements were obtained free from hysteresis. This involved keeping sweep rates low (typically about 1 V/min) and introducing a 3 s delay between changing voltage and reading current. The devices remained in an atmosphere of low-pressure (~10 mbar) helium during measurements. Examples of temperature-dependent current-voltage curves are shown in Fig. 2.

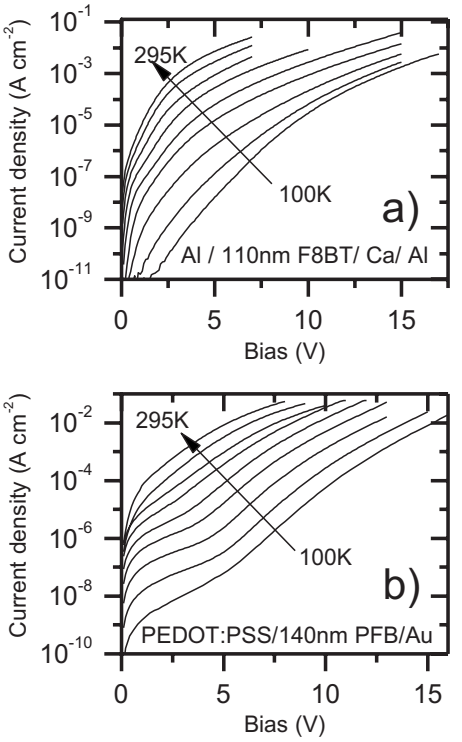

FIG. 2. Example current-voltage curves for (a) a 110-nm-thick F8BT electron-only device and (b) a 140-nm-thick PFB hole-only device at temperatures from 100 to 295 K (solid lines in order from bottom to top: 100, 125, 150, 175, 200, 225, 250, 275, and 295 K).

IV. DRIFT-DIFFUSION MODEL

A one-dimensional continuum model was used to simulate steady-state current-voltage curves in single-carrier devices. The model is quantitatively very similar to the model employed by van Mensfoort and Coehoorn, although we use a different iteration algorithm, more similar to that used by Koster *et al.*[25] Current density, *J*, is described by drift and diffusion of carriers in the standard way,

$$J = -\mu n e E + e D \frac{dn}{dx}, \tag{5}$$

$$\frac{dE}{dx} = \frac{e}{\varepsilon} n, \tag{6}$$

and

$$V = -\int_0^d E dx, \tag{7}$$

where *x* is the depth in the polymer film, *D* is the diffusion coefficient, and *e* is the charge of a single carrier. Equation (5) describes the current density in terms of the drift and diffusion currents. Equation (6) is Poisson's equation while Eq. (7) describes the application of a bias voltage. The equations are solved simultaneously to reach a steady-state solution in which $dJ/dx=0$.

The above equations are the standard drift-diffusion equations, which are commonly used to describe charge transport in organic semiconductors. In many previous studies, these are solved by using a constant mobility and applying the Boltzmann approximation ($D=\mu k_B T/e$), which, for semiconductors with a broad density of states, is accurate only in the low-carrier-density limit. These solutions are more appropri-

ate to crystalline semiconductors than disordered organic semiconductors. Here, we aim to solve the equations in the context of the EGDM. This is done by making three modifications to the standard drift-diffusion model. First, the shape of the Gaussian density of states is taken into account by using the generalized Einstein relation, as described by Roichman and Tessler.[26] This introduces a carrier-density-dependent enhancement factor, g_3, to the diffusion coefficient,

$$D(n,T) = \frac{g_3(n,T)\mu k_B T}{e}. \tag{8}$$

In the case of a Gaussian density of states, this factor is

$$g_3(n,T) = \frac{\int_{-\infty}^{\infty} \exp\left[-\frac{\xi^2}{2\hat{\sigma}}\right] \frac{1}{1+\exp(\xi-\xi_F)} d\xi}{n}, \tag{9}$$

where ξ_F is the relative quasi-Fermi level divided by $k_B T$, which can be evaluated from the Fermi distribution,

$$n = \int_{-\infty}^{\infty} \exp\left[-\frac{\xi^2}{2\hat{\sigma}}\right] \frac{\exp(\xi-\xi_F)}{1+\exp(\xi-\xi_F)} d\xi. \tag{10}$$

Second, the carrier-concentration dependence of mobility is included by introducing the density-dependent mobility enhancement factor $g_2(n,T)$ as in Eq. (4). We have tried using both the Pasveer[19] and Fishchuk[20] models to describe this factor. Both models assume that charge transport occurs by hopping with a Miller-Abrahams[27] hopping rate between sites with random energetic disorder. The Pasveer model gives a parameterization of results of numerical simulations of hopping behavior and is simple to apply

$$g_2(n,T) = \exp\left[\frac{1}{2}(\hat{\sigma}^2 - \hat{\sigma})\left(2\frac{n}{N_0}\right)^{\delta}\right], \tag{11}$$

$$\delta = 2\frac{\ln(\hat{\sigma}^2 - \hat{\sigma}) - \ln(\ln 4)}{\hat{\sigma}^2}, \tag{12}$$

where N_0 is the total density of states per unit volume. The Fishchuk model is more complicated to apply. It works by performing integrals of the hopping rate over the density of states in an effective-medium approach and is a function of the same parameters. Despite the different approaches, the two models produce quantitatively similar results. To reduce computation time, the functions $g_3(n,T)$ and $g_2(n,T)$ were evaluated before the start of the simulations and applied as look-up tables.

Finally, the electric field dependence of mobility is introduced by including the field-dependent mobility enhancement factor, $g_1(E,T)$, as in Eq. (2). Pasveer *et al.*[19] derived an alternative field-dependent expression in their model, which, as noted by Coehoorn *et al.*,[28] is quite dissimilar from the Poole-Frenkel-type field dependence that we have used. As discussed later in this paper, we have tried using this expression for g_1 but the agreement with our experimental data was found to be considerably worse than with the Poole-Frenkel-type expression. The use of the Poole-Frenkel-type field dependence and the Fishchuk concentration dependence are the most significant differences between our model and van Mensfoort's model, which uses the Pasveer model for both g_1 and g_2.

We treat all contacts as Ohmic with no injection barriers by fixing the carrier concentration at the boundaries according to thermal equilibrium $[n(0)=n(d)=N_0/2]$. A significant amount of band bending occurs implicitly at the contacts when using these boundary conditions,[29] causing carrier density to fall rapidly between the contact and the first few nanometers of polymer. The film was discretized into 300 grid points, calculating the field, carrier density, and current density at each point. The mobility is also calculated at each grid point according to the local electric field and carrier density. A site density of $N_0=10^{21}$ cm^{-3} was assumed.

V. FITTING RESULTS

For each temperature, *J-V* curves were simulated using the analytical expression for SCL current with Poole-Frenkel field dependence [Eq. (3)] for all thicknesses of device measured. A dielectric constant of 3.5 was assumed and the built-in voltage was assumed to be zero. The curves were fitted to experimental data by varying the free parameters μ_0 and γ using a least-squares fitting algorithm on a logarithmic scale. The same values of μ_0 and γ were shared between devices with different thicknesses. The best-fit curves for 295, 150, and 100 K temperatures are shown in Figs. 3(a)–3(c) for PFB and Figs. 4(a)–4(c) for F8BT. While reasonable fits are achieved at room temperature, an increasingly poor fit results as the temperature is reduced. In particular, a clear thickness dependence of the fit is observed, as the experimental current density is higher than predicted in thin polymer devices.

The fitting process was repeated using the drift-diffusion simulation detailed above. The simulations were run using both the Pasveer concentration-dependence model and the Fishchuk concentration dependence. Since each model requires an energetic disorder parameter, σ, to be defined, the fitting process was repeated using values of $\sigma=75$, 90, 100, and 110 meV. The best-fit curves for 75 and 100 meV disorder are shown in Fig. 3, and Figs. 4(d)–4(f) for the Fishchuk model and Figs. 4(g)–4(i) for the Pasveer model.

In both models, an increase in the level of disorder leads to increasing influence of the concentration-dependent term, g_2. This causes not only a large difference between best-fit values for μ_0 from different models at low temperatures but also an enhancement in simulated current density in thinner devices due to the larger carrier densities found in them. The latter of these effects corrects for the thickness dependence observed with the analytical fit, resulting in very good agreement between simulation and experiment at all temperatures. The best fits were achieved with the Pasveer concentration dependence with $\sigma=100$ meV for F8BT and 110 meV for PFB. The Fishchuk model has slightly weaker concentration dependence, requiring slightly larger values of disorder (by $\sim$10 meV) for a good fit, although good fits could be achieved with both models. Assuming that the carrier-concentration-dependent models are valid, the thickness dependence of the low-temperature *J-V* curves therefore pro-

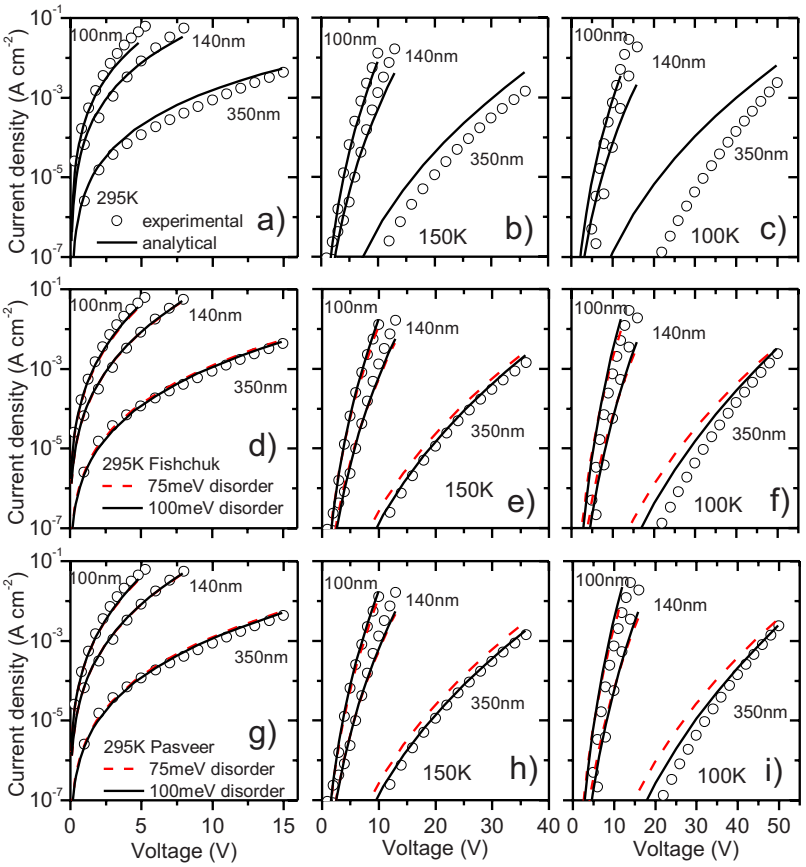

FIG. 3. (Color online) Best-fit curves for 100, 140, and 350 nm PFB devices. (a)–(c) fitted with analytical model, (d)–(f) fitted by numerical simulation using Fishchuk concentration-dependent mobility, and (g)–(i) numerical simulation with Pasveer concentration dependence. (a), (d), and (g) at 295 K; (b), (e), and (h) at 150 K, and (c), (f), and (i) at 100 K.

vides us with a tool for estimating the amount of disorder in the polymers by choosing the value of disorder that gives us the best fit across different thicknesses.

Interestingly, recent work by Steyrleuthner *et al.*[4] was able to successfully describe electron transport in F8BT using an alternative model based on trap-limited transport instead of Gaussian disorder. The model[30] assumes that the material contains a number of trapping sites characterized by an exponential energy distribution. An apparent carrier-density dependence of mobility arises as trap sites become full at high concentrations. The characteristic energy of the trap distribution used to best describe transport in F8BT in this work was 100 meV, the same as the width of disorder used in our model to best describe the same material. Although the models are considerably different, they arrive at the same conclusion that electron transport in F8BT is dominated by localized transport between states with a distribution of energies of 100 meV characteristic width. The exact nature of transport between these sites appears to be less important than the characteristic energy.

Implementations of the GDM with Miller-Abrahams hopping rates predict a temperature dependence for mobility in the low-carrier-concentration limit of the form

$$\mu_0(T) = \mu_\infty \exp[-c\hat{\sigma}^2], \tag{13}$$

for mobility, where μ_∞ is the high-temperature limit of mobility and c is a constant. The value of c is slightly dependent on the degree of carrier localization used in the simulations.[28] Localization is characterized by the ratio of the carrier localization length, b, to the intersite distance, a. Generally, for disordered organic semiconductors, it is assumed that b/a is about 1/10. Using this value, c is equal to 0.44 for Bässler's model,[18] 0.42 in Pasveer's model[19] and 0.48 for Fishchuk's.[20] Figure 5 shows the best-fit values of μ_0 as a function of $1/T^2$ for different values of disorder. The solid lines show best fits to expression (13), with the parameters shown in Table I. The above temperature dependence is indeed observed for the values of disorder that gave the best fit to the thickness-dependent J-V curves over the complete range of temperatures from room temperature to 100 K. Values of c shown in Table I are in reasonable agreement with the above values for disorders of 100 and 110 meV, suggesting that the assumed ratio of $b/a=1/10$ is reasonable for modeling PFB and F8BT.

We found that a good fit to expression (13) was achieved for a range of values of σ, all giving reasonable values of c. The temperature dependence alone is insufficient for determining the amount of disorder in the materials. It is apparent, then, that both thickness-dependent measurements and a wide range of temperatures are necessary for deriving σ with confidence. Even then, we qualify our values of σ with at least 10 meV of uncertainty.

While mobilities derived from numerical fitting with the GDM produced a T^{-2} temperature dependence, the mobilities derived by fitting with the analytical expression (3), shown in Fig. 6(a), instead have an Arrhenius temperature dependence between about 150 K and room temperature. Activation energies of 330 and 370 meV were obtained for PFB and F8BT, respectively. Craciun *et al.*[21] also found experimen-

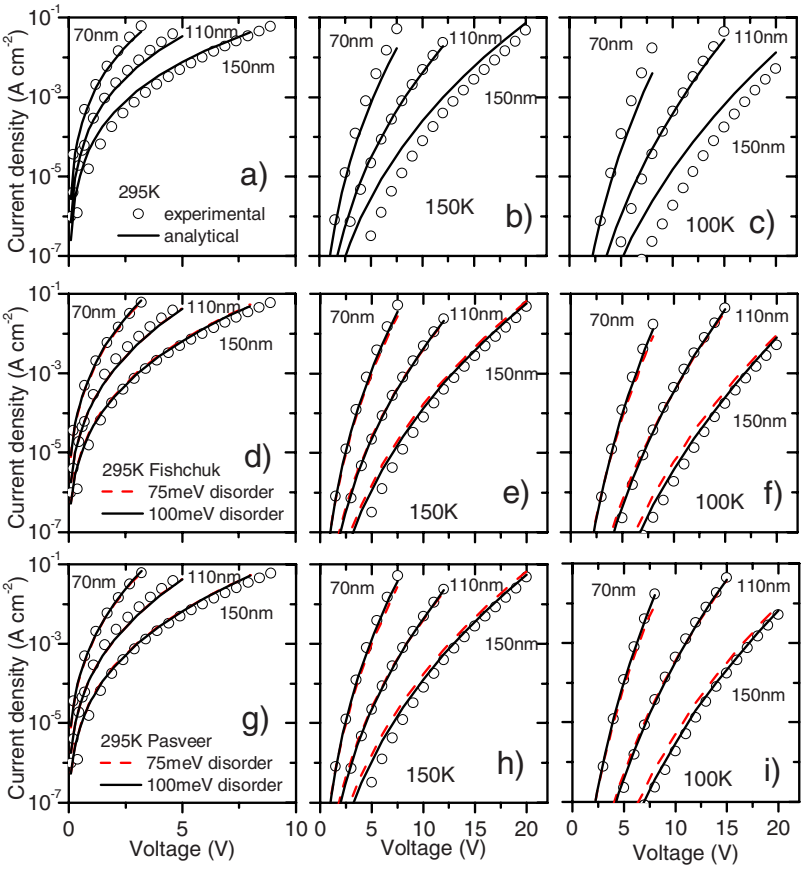

FIG. 4. (Color online) Best-fit curves for 70, 110, and 150 nm F8BT devices. (a)–(c) fitted with analytical model, (d)–(f) fitted by numerical simulation using Fishchuk concentration-dependent mobility, and (g)–(i) numerical simulation with Pasveer concentration dependence. (a), (d), and (g) at 295 K; (b), (e), and (h) at 150 K, and (c), (f), and (i) at 100 K.

tally an Arrhenius temperature dependence for mobility in a wide range of materials when fitting data using the same analytical expression. The explanation is that the analytical model measures an effective mobility,[23] $\mu_{eff}(T) = \mu_0(T) g_2(n,T)$, at a finite carrier concentration and is different in definition from the zero-field, zero carrier-density concentration mobility, $\mu_0(T)$, measured by fitting with the full simulation. This behavior is expected according to the observation of Fishchuk[20] that the mobility tends to Arrhenius behavior at high carrier concentrations in the GDM. Caution should be exercised when applying such an effective mobility to different device configurations in which the carrier density is likely to be very different. Figure 6(b) compares the effective mobilities extracted analytically with the mobilities from the best-fitting numerical simulations. Due to the enhancement effect of g_2, the former mobilities are considerably higher than the latter.

By simulating *J-V* curves, we are able to assess the relative importance of the different mobility enhancement factors. At room temperature, we found that the field-dependent term, g_1, was generally of much greater importance than the carrier-concentration dependence, g_2. For example, in a 150-

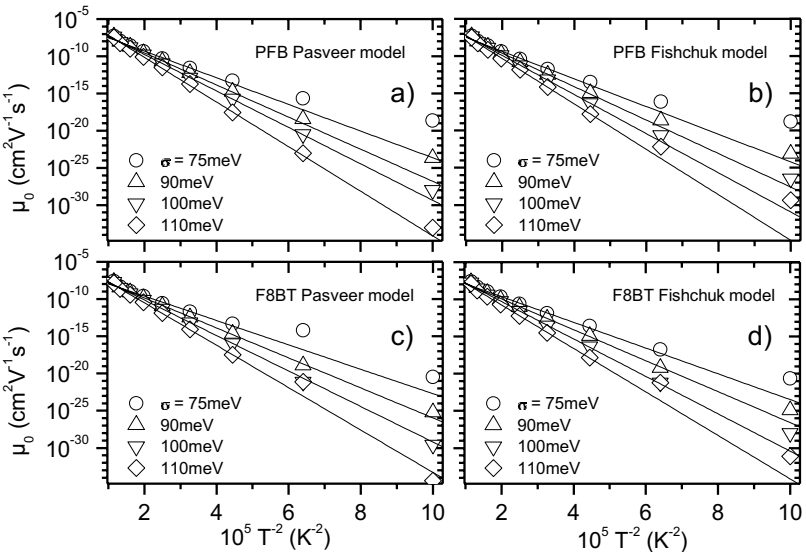

FIG. 5. Best-fit mobility values derived from numerical simulations. (a) PFB with Pasveer concentration dependence, (b) PFB with Fishchuk concentration dependence, (c) F8BT with Pasveer, and (d) F8BT with Fishchuk. Symbols: mobilities derived for each temperature and each value of disorder. Solid lines: best-fit lines according to expression (10).

TABLE I. Parameters describing the temperature dependence of mobility fitted with different levels of disorder.

σ (meV)	μ_∞ PFB ($cm^2\ V^{-1}\ s^{-1}$)		μ_∞ F8BT ($cm^2\ V^{-1}\ s^{-1}$)		c PFB		c F8BT	
	Pasveer	Fishchuk	Pasveer	Fishchuk	Pasveer	Fishchuk	Pasveer	Fishchuk
75	1.9×10^{-6}	2.4×10^{-6}	4.7×10^{-7}	6.8×10^{-7}	0.53	0.56	0.49	0.53
90	6.0×10^{-6}	7.6×10^{-6}	1.5×10^{-6}	1.7×10^{-6}	0.46	0.47	0.43	0.44
100	1.3×10^{-5}	2.2×10^{-5}	4.5×10^{-6}	5.4×10^{-6}	0.42	0.45	0.41	0.43
110	6.8×10^{-5}	3.8×10^{-5}	1.5×10^{-5}	1.2×10^{-5}	0.42	0.43	0.40	0.41

nm-thick F8BT film, the inclusion of the g_1 term in the mobility equation caused a factor of 8 increase in current density at 1 V, whereas g_2 only contributes a factor of 1.5 and g_3 1.3. At low temperatures, the concentration dependence is much more important, with current-density enhancements of 11, 23, and 1.8 for g_1, g_2, and g_3, respectively for the same situation at 200 K. Therefore, a study of the form of the field dependence at high temperatures is of great importance.

Figure 7(a) shows the experimental current density in a 150-nm-thick F8BT device normalized by the square of the mean electric field (V/d) plotted against the square root of the mean electric field. According to the Murgatroyd expression (3), the result should be a straight line if Poole-Frenkel-type field dependence is observed and concentration-dependent effects are small. Here this behavior is obeyed at fields down to 5×10^4 V/cm, below which anomalies due to possible small finite built-in potential and carrier-injection effects cause some uncertainty. This is in agreement with the general observation that this field dependence is observed in most organic semiconductors over a wide field range. Solid lines in Fig. 7(a) correspond to simulated J-V curves using Pasveer concentration dependence with Poole-Frenkel field dependence and 100 meV disorder. We repeated the fitting experiment using the Pasveer field dependence instead of Poole-Frenkel. In this case, the free parameter, γ, is no longer used. Instead, the Pasveer model is strongly dependent on the intersite distance, a, so we allowed this parameter to vary in our fitting (with $N_0=a^{-3}$). Best fits were obtained with a of about 3 nm, a value which is rather large compared with the hopping distances normally expected in conjugated polymers. The resulting curves are shown as dashed lines in Fig. 7(a). It is clear that the Poole-Frenkel expression results in a much better fit to our data.

Monte Carlo transport simulations using the GDM predict Poole-Frenkel field dependence only at strong fields ($E>5\times10^5$ V/cm). Instead, simulations using spatially correlated disorder[31–34] have been found to predict Poole-Frenkel behavior extending to lower electric fields. Such models predict a temperature dependence of $\gamma\propto T^{-\alpha}$, where α varies between models but can be expected to lie between 1 and 2 depending on the degree of correlation, with completely uncorrelated disorder giving about 2. Figure 7(b) shows values

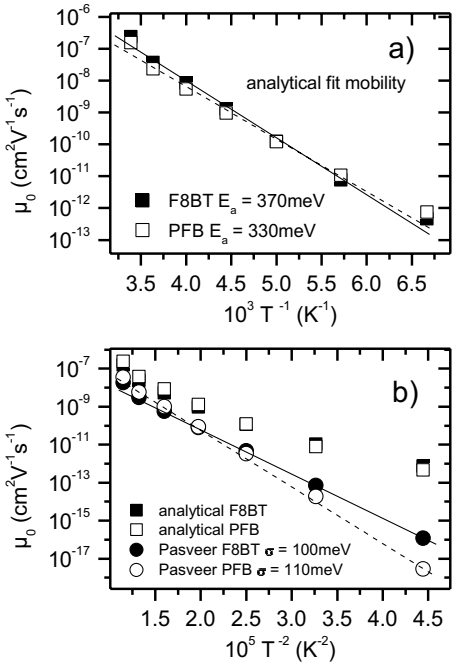

FIG. 6. (a) Best-fitting mobilities used for fitting the analytical Murgatroyd expression (3) for SCL current on an Arrhenius plot for F8BT (solid line) and PFB (dotted line). (b) Best-fit mobilities from analytical model compared with best-fit mobilities from numerical simulations using Pasveer concentration dependence and 100 meV disorder for F8BT and 110 meV disorder for PFB, with best-fit curves to expression (10) for F8BT (solid line) and PFB (dashed line)

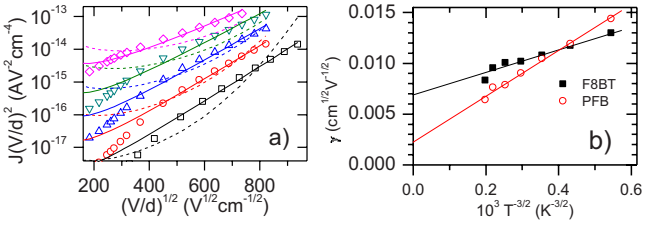

FIG. 7. (Color online) (a) The field dependence of normalized space-charge limited current in 150-nm-thick F8BT devices. Symbols are experimental results: squares 200 K, circles 225 K, up triangles 250 K, down triangles 275 K, and diamonds 295 K. Solid lines are best fits with Poole-Frenkel field dependence and Pasveer concentration dependence and dashed lines are best fits with the full Pasveer EGDM for field and concentration dependence. (b) Temperature dependence of γ derived from fitting F8BT with 100 meV disorder and PFB with 110 meV disorder using Pasveer concentration dependence and Poole-Frenkel field dependence. Solid lines: best fit with $\gamma\propto T^{-1.5}$.

of γ obtained from the simulated best fits. The figure shows a reasonable fit to a temperature dependence of $\alpha=1.5$ (solid lines), suggesting that correlated disorder might explain the observed field dependence in PFB and F8BT. Recently the EGDM was modified to include the effects of correlated disorder using the same methods as Pasveer *et al.*, resulting in the extended correlated disorder model (ECDM).[34] This model was used to study the mobility of holes in a PFB-like polymer,[35] whereupon it was concluded that both EGDM and ECDM provided a good fit to experiments, although the EGDM was the preferred model as the ECDM required an unrealistically high site density for a good fit. Our results appear to counter this view, as they suggest that some form of correlated disorder is necessary to fully explain the field dependence. Between these two studies, the appropriate use of correlated disorder still remains an unresolved issue.

VI. CONCLUSIONS

We have implemented a model that can successfully predict the temperature and thickness dependence of SCL charge transport in PFB and F8BT without needing to include specific trapping sites. This is especially significant in the case of electron transport in F8BT as most previous attempts to model electron transport in conjugated polymers have described steady-state currents as being a trap-limited process.[4,5,36] We found that hole transport in PFB could be modeled using a Gaussian disorder of 110 ± 10 meV and electron transport in F8BT with 100 ± 10 meV disorder. The amount of disorder in F8BT is the same as the width of trap energies used to describe electron transport in a previous work,[4] suggesting that trap-limited behavior and Gaussian disorder share many features in the underlying physics. The use of a Gaussian disorder reduces the effects of many processes (for example, local energetic variations due to dipoles, chain distortions, impurities, and trapping effects) to a single disorder parameter without describing them explicitly. By reducing a number of unknown properties to a single value, it provides a simple yet adequate model for describing transport behavior in a range of complex disordered systems and can be included in device models with the inclusion of a minimal set of empirical parameters.

We have confirmed that the EGDM works over a wider range of temperatures than has previously been used. It was also found that both Pasveer and Fishcuk models of carrier-concentration dependence can be used. However, the Pasveer description of the field dependence of mobility did not work for either material and a Pool-Frenkel-type field dependence was used instead. This suggests that correlated disorder might play a role in transport in these materials.

We also confirmed the previously made observation[23] that a simple analytical analysis of SCL current densities measures an effective mobility that has an Arrhenius temperature dependence. However, this effective mobility varies as a function of device thickness. Caution should be exercised with such effective mobilities, as real carrier mobilities can differ by orders of magnitude when different electric fields and carrier densities are used.

ACKNOWLEDGMENTS

This work was supported by the European Commission Framework Programme 6 project MODECOM (Grant No. NMP-CT-2006-016434). Polymers were supplied by Cambridge Display Technology Ltd.

*Present address: University of Potsdam, Institute of Physics and Astronomy, Karl-Liebknecht Strasse 24-25, Building 28, D-14476 Potsdam-Golm, Germany; james.blakesley@physics.org

[1] A. B. Walker, A. Kambili, and S. J. Martin, J. Phys.: Condens. Matter **14**, 9825 (2002).
[2] P. W. Blom, V. D. Mihailetchi, L. J. A. Koster, and D. E. Markov, Adv. Mater. (Weinheim, Ger.) **19**, 1551 (2007).
[3] S. R. Tseng, Y. S. Chen, H. F. Meng, H. C. Lai, C. H. Yeh, S. F. Horng, H. H. Liao, and C. S. Hsu, Synth. Met. **159**, 137 (2009).
[4] R. Steyrleuthner, S. Bange, and D. Neher, J. Appl. Phys. **105**, 064509 (2009).
[5] M. M. Mandoc, B. de Boer, G. Paasch, and P. W. M. Blom, Phys. Rev. B **75**, 193202 (2007).
[6] A. C. Morteani, A. S. Dhoot, J.-S. Kim, C. Silva, N. C. Greenham, C. Murphy, E. Moons, S. Ciná, J. H. Burroughes, and R. H. Friend, Adv. Mater. (Weinheim, Ger.) **15**, 1708 (2003).
[7] C. McNeill, S. Westenhoff, C. Groves, R. H. Friend, and N. C. Greenham, J. Phys. Chem. C **111**, 19153 (2007).
[8] V. D. Mihailetchi, J. K. J. van Duren, P. W. M. Blom, J. C. Hummelen, R. A. J. Janssen, J. M. Kroon, M. T. Rispens, W. J. H. Verhees, and M. M. Wienk, Adv. Funct. Mater. **13**, 43 (2003).
[9] N. F. Mott and R. W. Gurney, *Electronic Processes in Ionic Crystals* (Oxford University Press, Oxford, 1940).
[10] L. B. Schein, A. Peled, and D. Glatz, J. Appl. Phys. **66**, 686 (1989).
[11] M. Redecker, D. D. C. Bradley, M. Inbasekaran, W. W. Wu, and E. P. Woo, Adv. Mater. (Weinheim, Ger.) **11**, 241 (1999).
[12] R. U. A. Khan, D. Poplavskyy, T. Kreouzis, and D. D. C. Bradley, Phys. Rev. B **75**, 035215 (2007).
[13] L. Bozano, S. A. Carter, J. C. Scott, G. G. Malliaras, and P. J. Brock, Appl. Phys. Lett. **74**, 1132 (1999).
[14] N. D. Nguyen, M. Schmeits, and H. P. Loebl, Phys. Rev. B **75**, 075307 (2007).
[15] P. N. Murgatroyd, J. Phys. D: Appl. Phys. **3**, 151 (1970).
[16] P. W. M. Blom, M. J. M. de Jong, and M. G. van Munster, Phys. Rev. B **55**, R656 (1997).
[17] C. Tanase, E. J. Meijer, P. W. M. Blom, and D. M. de Leeuw, Phys. Rev. Lett. **91**, 216601 (2003).
[18] H. Bässler, Phys. Status Solidi B **175**, 15 (1993).
[19] W. F. Pasveer, J. Cottaar, C. Tanase, R. Coehoorn, P. A. Bobbert, P. W. M. Blom, D. M. de Leeuw, and M. A. J. Michels, Phys. Rev. Lett. **94**, 206601 (2005).
[20] I. I. Fishchuk, V. I. Arkhipov, A. Kadashchuk, P. Heremans, and H. Bässler, Phys. Rev. B **76**, 045210 (2007).
[21] N. I. Craciun, J. Wildeman, and P. W. M. Blom, Phys. Rev. Lett.

100, 056601 (2008).
[22] S. L. M. van Mensfoort and R. Coehoorn, Phys. Rev. B **78**, 085207 (2008).
[23] S. L. M. van Mensfoort, S. I. E. Vulto, R. A. J. Janssen, and R. Coehoorn, Phys. Rev. B **78**, 085208 (2008).
[24] J. J. M. van der Holst, M. A. Uijttewaal, and B. Ramachandhran, Phys. Rev. B **79**, 085203 (2009).
[25] L. J. A. Koster, E. C. P. Smits, V. D. Mihailetchi, and P. W. M. Blom, Phys. Rev. B **72**, 085205 (2005).
[26] Y. Roichman and N. Tessler, Appl. Phys. Lett. **80**, 1948 (2002).
[27] A. Miller and E. Abrahams, Phys. Rev. **120**, 745 (1960).
[28] R. Coehoorn, W. F. Pasveer, P. A. Bobbert, and M. A. J. Michels, Phys. Rev. B **72**, 155206 (2005).
[29] J. C. Blakesley and N. C. Greenham, J. Appl. Phys. **106**, 034507 (2009).
[30] P. Mark and W. Helfrich, J. Appl. Phys. **33**, 205 (1962).
[31] Yu. N. Gartstein and E. M. Conwell, Chem. Phys. Lett. **245**, 351 (1995).
[32] S. V. Novikov, D. H. Dunlap, V. M. Kenkre, P. E. Parris, and A. V. Vannikov, Phys. Rev. Lett. **81**, 4472 (1998).
[33] Z. G. Yu, D. L. Smith, A. Saxena, R. L. Martin, and A. R. Bishop, Phys. Rev. B **63**, 085202 (2001).
[34] M. Bouhassoune, S. L. M. van Mensfoort, P. A. Bobbert, and R. Coehoorn, Org. Electron. **10**, 437 (2009).
[35] R. J. de Vries, S. L. M. van Mensfoort, V. Shabro, S. I. E. Vulto, R. A. J. Janssen, and R. Coehoorn, Appl. Phys. Lett. **94**, 163307 (2009).
[36] D. Poplavskyy, W. Su, and F. So, J. Appl. Phys. **98**, 014501 (2005).